Inorganic Chemistry
Article

Inorg. Chem. **2011**, *50*, 771–782 **771**
DOI: 10.1021/ic100759h

Comparative Study of Mono- and Dinuclear Complexes of Late 3d-Metal Chlorides with *N,N*-Dimethylformamide in the Gas phase†

Lucie Ducháčková,‡ Jana Roithová,*,‡ Petr Milko,†,§ Jan Žabka,∥ Nikos Tsierkezos,⊥ and Detlef Schröder*,†

†*Institute of Organic Chemistry and Biochemistry, Flemingovo nám. 2, 16610 Prague 6, Czech Republic,* ‡*Department of Organic Chemistry, Charles University in Prague, Hlavova 8, 12843 Prague 2, Czech Republic,* §*Institute of Chemistry and the Lise-Meitner-Minerva Center for Computational Quantum Chemistry, Hebrew University of Jerusalem, 91904, Jerusalem, Israel,* ∥*J. Heyrovský Institute of Physical Chemistry, Dolejškova, 3, 18223 Prague 8, Czech Republic, and* ⊥*Institut für Chemie, Elektrochemie und Galvanotechnik, Technische Universität Ilmenau, Weimarer Strasse 25, 98693 Ilmenau, Germany*

Received April 20, 2010

Mono- and binuclear complexes of *N,N*-dimethylformamide (DMF) with chlorides of the divalent, late 3d metals M = Co, Ni, Cu, and Zn are investigated by means of electrospray ionization (ESI). Specifically, ESI leads to monocations of the type $[(DMF)_nMCl]^+$ and $[(DMF)_nM_2Cl_3]^+$, of which the species with $n = 2$ and 3 were selected for in-depth studies. The latter include collision-induced dissociation experiments, gas-phase infrared spectroscopy, and calculations using density functional theory. The mononuclear complexes $[(DMF)_nMCl]^+$ almost exclusively lose neutral DMF upon collisional activation with the notable exception of the copper complex, for which also a reduction from Cu^{II} to Cu^{I} concomitant with the release of atomic chlorine is observed. For the dinuclear clusters, there exists a competition between loss of a DMF ligand and cluster degradation via loss of neutral MCl_2 with decreasing cluster stability from cobalt to zinc. For the specific case of $[(DMF)_nZnCl]^+$ and $[(DMF)_nZn_2Cl_3]^+$, ion-mobility mass spectrometry indicates the existence of two isomeric cluster ions in the case of $[(DMF)_2Zn_2Cl_3]^+$ which corroborates parallel theoretical predictions.

Introduction

The coordination of metal ions to biomolecules is of considerable interest and has been involved as an essential factor in several diseases (e.g., Alzheimer).[1] Closely related with the formation of metal/ligand complexes is ion solvation and element speciation in pure and mixed solvents. A wide variety of experimental techniques is available for the investigation of ions in solution, yet the conclusions which can be drawn with respect to the identity of the molecular species being present are often only very indirect.[2] Spectroscopic methods such as nuclear magnetic resonance, as the most powerful tools for the structural analysis of small molecules in solution, also do not provide clear insight because of the rapid dynamic equilibria in salt solutions such that only averaged properties are sampled. Hence it appears as a potential useful addition to the methodological repertoire to extend the solution techniques by mass spectrometric measurements of ionic species formed from solutions upon electrospray ionization (ESI).[3,4] From a conceptual point of view, the situation is reverse in gas-phase studies because the identification of the (charged) molecular species is facile, whereas the correlation of the species observed in the gas phase with the situation in bulk solution is only indirect. It is in fact still under debate, if ESI experiments can be used to reproduce or even predict solution phenomena,[5] but at least for the rapid equilibria in aqueous solutions of metal salts first quantitative correlations between the condensed and the gaseous phase have been proposed.[6,7] In the context of earlier electrospray experiments in this direction, *N,N*-dimethylformamide (DMF) has been chosen as a simple model for the interaction of metal ions with amide groups and as a prototype of a common aprotic polar solvent.[8] In terms of the

† Dedicated to František Tureček on the occasion of his 60th birthday.

*To whom correspondence should be addressed. E-mail: roithova@natur.cuni.cz (J.R.), detlef.schroeder@uochb.cas.cz (D.S.).

(1) Jobling, M. F.; Huang, X.; Stewart, L. R.; Barnham, K. J.; Volitakis, I.; Perugini, M.; White, A. R.; Cherny, R. A.; Masters, C. L.; Barrow, C. J.; Collins, S. J.; Bush, A. I.; Cappai, R. *Biochemistry* **2001**, *40*, 8073.

(2) (a) Hefter, G.; Marcus, Y.; Waghorne, W. E. *Chem. Rev.* **2002**, *102*, 2773. (b) Marcus, Y.; Hefter, G. *Chem. Rev.* **2004**, *104*, 3405.

(3) (a) Yamashita, M.; Fenn, J. B. *J. Phys. Chem.* **1984**, *88*, 4451. (b) Fenn, J. B. *J. Am. Soc. Mass Spectrom.* **1993**, *4*, 524.

(4) Jayaweera, P.; Blades, A. T.; Ikonomou, M. G.; Kebarle, P. *J. Am. Chem. Soc.* **1990**, *112*, 2452.

(5) Di Marco, V. B.; Bombi, G. G. *Mass Spectrom. Rev.* **2006**, *25*, 347.

(6) Cheng, Z. L.; Siu, K. W. M.; Guevremont, R.; Berman, S. S. *J. Am. Soc. Mass Spectrom.* **1992**, *3*, 281.

(7) (a) Walther, C.; Fuss, M.; Büchner, S. *Radiochim. Acta* **2008**, *96*, 411. (b) Urabe, T.; Tsugoshi, T.; Tanaka, M. *J. Mass. Spectrom.* **2009**, *44*, 193. (c) Tsierkezos, N. G.; Roithová, J.; Schröder, D.; Ončák, M.; Slavíček, P. *Inorg. Chem.* **2009**, *48*, 6287.

Published on Web 12/28/2010

fundamental processes occurring in ESI of aqueous salt solutions, the behavior of DMF is quite typical in that as a good donor ligand it replaces the water ligands in hydrated cations such as $[M(H_2O)_n]^{m+}$ or $[M(X)(H_2O)_n]^{(m-1)+}$ (X = monovalent counterion, e.g., a halide) to afford the corresponding DMF-ligated complexes.[9,10] As a side aspect of these studies it has been found that DMF and also other nitrogen-based ligands[11,12] promote the formation of oligonuclear metal complexes, which might also have important implications for the role of the ligands (or solvents) in transition-metal catalysis.[13] In the specific case of the dinuclear nickel(II) chloride $[(DMF)_2Ni_2Cl_3]^+$, also the involvement of isomeric cluster structures has been suggested.[11] With regard to the more general relevance of these studies beyond the specific field of gas-phase ion chemistry, we refer to recent mass-spectrometric studies about the mechanism of the Cu^{II}-mediated coupling of naphthol to bisnaphthol;[12] the latter compound is one of the most versatile chiral catalysts.[14] For this reaction, gas-phase experiments clearly suggest that the decisive C−C-coupling proceeds via dinuclear copper clusters stabilized by nitrogen ligands.[15] This proposal has meanwhile also been appreciated in the synthetic community,[16] and it resolved previous uncertainty about the mechanism of the Cu^{II}-mediated naphthol coupling.[17] Besides being a versatile solvent, DMF is also an important nitrogen ligand with regard to the aggregation of metal ions[18,19] and the stabilization of catalytically active metal clusters.[20−22] As a recent example for the effect of DMF on ion aggregation, we refer to the observation of Sarma et al. that mononuclear pyrazolato zinc carboxylate complexes convert into dinuclear clusters in the presence of DMF.[23]

Here, we report a comparative study of selected mono- and dinuclear DMF complexes of the metal(II) chlorides MCl_2 with M = Co, Ni, Cu, and Zn. DMF is chosen as a ligand because it is known as a well coordinating ligand of transition metals, while not being as basic as aliphatic amines, which may cause precipitation of metal hydroxides from aqueous solutions.[24] Moreover, metal-ion coordination to DMF might be associated with structurally sensitive property changes of the resulting complexes as a function of the metal and its valence state. The monocationic species $[(DMF)_nMCl]^+$ and $[(DMF)_nM_2Cl_3]^+$, respectively, formed upon ESI of the various sample solutions were investigated experimentally by collision experiments, infrared spectroscopy of the gaseous ions, and ion mobility studies in the case of the zinc complexes. For the mononuclear ions and the dinuclear zinc clusters, the experimental work is complemented by theoretical studies using density functional theory (DFT).

Experimental Details

The experiments were performed with a TSQ Classic mass spectrometer which has been described previously.[25] Briefly, the TSQ Classic consists of an ESI source combined with a tandem mass spectrometer of QOQ configuration (Q stands for quadrupole and O for octopole). The ions were generated by infusion of methanol/water (1:1) solutions of the corresponding metal(II) chlorides (ca. 10^{-3} mol l^{-1}) with 1% DMF to the ESI source using a syringe pump at a flow rate of 5 μL min^{-1}. The temperature of the heated capillary was maintained 200 °C. We note in passing that DMF should not have been dried over a molecular sieve because this leads to a substantial contamination by alkali ions which prevent a quantitative analysis of the source spectra.

In ESI, the size of the generated metal-ion solvates $ML_n^{\pm}$ very much depends on the source conditions, which can be varied from very soft (large n) to moderate (medium values of n) to hard (n = 0, 1).[26,27] For the generation of the species discussed below, medium conditions were applied; that is, the potentials at the end of the transfer capillary and at the first focal lens were adjusted to −10 V and +10 V, respectively. In addition to DMF-containing ions, in the case of $CuCl_2$/DMF/H_2O, this leads to $[(H_2O)_nCuX]^+$ ions (X = OH and Cl) with average hydration numbers (n_{av}) of about 3.5 (see below). The first quadrupole was used as a mass filter to scan mass spectra of the ions produced or to select the ions of interest. For CID, the mass-selected ions were guided through the octopole serving as a collision chamber followed by mass analysis of the ionic reaction products by means of the second quadrupole and subsequent detection. Xenon was used as a collision gas at typical pressures of $0.3-2 \times 10^{-4}$ mbar, where the lower boundary of this range corresponds to approximate single-collision conditions.[27] Using a previously described approximate method based on sigmoid functions of the type $I_i(E_{CM}) = (BR_i/(1+e^{(E_{1/2,i}-E_{CM})b_i}))$,[28] phenomenological appearance energies (*AEs*) are derived from the energy dependences of the product distributions in the CID spectra. Here, BR_i stands for the branching ratio of a particular product ion ($\sum BR_i = 1$), $E_{1/2}$ is the energy at which the sigmoid function has reached half of its maximum, E_{CM} is the collision energy in the center-of-mass frame ($E_{CM} = z \times m_T/(m_T+m_I) \times E_{lab}$, where z is the ion's charge, m_T and m_I stand for the masses of the collision gas and the ion, respectively),

(8) For a review of metal-amide complexes in the condensed phase, see: Clement, O.; Rapko, B. M.; Hay, B. P. *Coord. Chem. Rev.* **1998**, *170*, 203.
(9) Tsierkezos, N.; Schröder, D.; Schwarz, H. *J. Phys. Chem. A* **2003**, *107*, 9575.
(10) Tsierkezos, N. G.; Roithová, J.; Schröder, D.; Molinou, I. E.; Schwarz, H. *J. Phys. Chem. B* **2008**, *112*, 4365.
(11) Tsierkezos, N. G.; Schröder, D.; Schwarz, H. *Int. J. Mass Spectrom.* **2004**, *235*, 33.
(12) (a) Roithová, J.; Schröder, D. *Chem.—Eur. J.* **2008**, *14*, 2180. (b) Roithová, J.; Milko, P. *J. Am. Chem. Soc.* **2010**, *132*, 281.
(13) Šrogl, J.; Hyvl, J.; Révész, A.; Schröder, D. *Chem. Comun.* **2009**, 3463.
(14) Brunel, J. M. *Chem. Rev.* **2005**, *105*, 857.
(15) For a recent review about diamine ligands in copper catalysis, see: Surry, D. S.; Buchwald, S. L. *Chem. Sci.* **2010**, *1*, 13.
(16) (a) Hewgley, J. B.; Stahl, S. S.; Kozlowski, M. C. *J. Am. Chem. Soc.* **2008**, *130*, 12232. (b) McGlacken, G. P.; Bateman, L. M. *Chem. Soc. Rev.* **2009**, *38*, 2447.
(17) (a) Hovorka, M.; Závada, J. *Tetrahedron* **1992**, *48*, 9517. (b) Smrčina, M.; Poláková, J.; Vyskočil, Š; Kočovský, P. *J. Org. Chem.* **1993**, *58*, 4534.
(18) Dance, I. G.; Garbutt, R. G.; Bailey, T. D. *Inorg. Chem.* **1990**, *29*, 603.
(19) Golubeva, E. N.; Kokorin, A. I.; Zubareva, N. A.; Vorontsov, P. S.; Smirnov, V. V. *J. Mol. Catal. A* **1999**, *146*, 343.
(20) (a) Tang, Q.; Zhang, Q.; Wu, H.; Wang, Y. *J. Catal.* **2005**, *230*, 384. (b) Pachón, L. D.; Thathagar, M. B.; Hartl, F.; Rothenberg, G. *Phys. Chem. Chem. Phys.* **2006**, *8*, 151. (c) Pastoriza-Santos, I.; Liz-Marzán, L. M. *Adv. Funct. Mater.* **2009**, *19*, 679.
(21) For a pronounced effect of DMF addition in copper-mediated trifluormethylations, also see: Dubnina, G. G.; Furutachi, H.; Vicic, D. A. *J. Am. Chem. Soc.* **2008**, *130*, 8600.
(22) For a spectacular sequence in Pd/Cu catalysis in which DMF and additional ammonia serve as a source of CN as a building block in C-H bond activation, see: Kim, J.; Chang, S. *J. Am. Chem. Soc.* **2010**, *132*, 10272.
(23) Sarma, R.; Kalita, D.; Baruah, J. B. *Dalton Trans.* **2009**, 7428.
(24) Schröder, D.; Schwarz, H.; Schenk, S.; Anders, E. *Angew. Chem., Int. Ed.* **2003**, *42*, 5087.
(25) (a) Roithová, J.; Schröder, D. *Phys. Chem. Chem. Phys.* **2007**, *9*, 713. (b) Roithová, J.; Schröder, D.; Mišek, J.; Stará, I. G.; Starý, I. *J. Mass Spectrom.* **2007**, *42*, 1233.
(26) Cech, N. B.; Enke, C. G. *Mass Spectrom. Rev.* **2001**, *20*, 362.
(27) Schröder, D.; Weiske, T.; Schwarz, H. *Int. J. Mass Spectrom.* **2002**, *219*, 729.
(28) Schröder, D.; Engeser, M.; Brönstrup, M.; Daniel, C.; Spandl, J.; Hartl, H. *Int. J. Mass Spectrom.* **2003**, *228*, 743.

and b (in eV^{-1}) describes the rise of the sigmoid curve and thus the phenomenological energy dependence. The collision energy in the laboratory frame is determined by the voltage offset ΔU_{oct} between the source and the octopole collision cell, that is, $E_{lab} = z \times e \times \Delta U_{oct}$. The zero point of the collision energy scale was determined by retarding potential analysis.[29] Further, the kinetic energy width of the incident beam (fwhm = ca. 1.3 eV in E_{lab}) is deconvoluted from the data. To this end, a sigmoid is derived which, after folding with a Gaussian having a half width of 1.3 eV, leads to the sigmoid derived from experiment.[30] We note, however, that for the systems under study, entropic effects and also kinetic shifts in ion dissociation will be of importance.[31] The appearance energies given below should thus only be considered as semiquantitative measures for the fragmentation behavior of the homologous complexes studied in this work. While the empirical fit using sigmoid functions is able to reproduce the measured ion yields for a broad variety of gaseous ions,[32] it is obvious that neither $E_{1/2}$ nor AE correspond to the intrinsic thermochemistry of the fragmentation of interest.[31] Notwithstanding these possible limitations of the method, it is certainly useful for the comparison of trends within series of homologous metal ions.[32]

In the case of the zinc system, additional exploratory experiments were performed with a SYNAPT G2 ion mobility instrument.[33,34] In brief, the instrument has an ESI source from which the ions are extracted toward a quadrupole mass filter for the selection of parent ions. In the ion-mobility mode, the mass-selected ions then enter an argon-filled linear ion trap in which they are collected and then admitted in pulses via a helium cooling cell to a drift tube in which nitrogen is present at an approximate pressure of 2 mbar. After extraction from the drift tube, the ions pass a transfer cell and enter the source region of a reflectron time-of-flight (TOF) mass spectrometer, which continuously records mass spectra with a mass resolution ($m/\Delta m$) of about 25000. In the ion-mobility experiments described below, the desired $[(DMF)_nZn_mCl_{2m-1}]^+$ cations (m = 1, 2; n = 1−3) were mass-selected using Q1 at unit mass resolution, and the ion mobility was recorded in time steps of about 0.04 ms required for recording and processing TOF spectra from m/z 50 to 600. To minimize fragmentation of the relatively weakly bound DMF complexes, the potentials in ion transfer to drift cell were lowered as much as possible, while still maintaining acceptable ion transmission.[35]

Gas-phase infrared spectra (IR) of mass-selected $[(DMF)_nMCl]^+$ and $[(DMF)_nM_2Cl_3]^+$ ions were recorded with a Bruker Esquire 3000 IT-MS[36−38] mounted to a beamline of the free electron laser at CLIO (Centre Laser Infrarouge Orsay, Orsay, France). The ions of interest were generated by ESI as described above and transferred to the ion trap. After mass selection, infrared multiphoton dissociation was induced by admittance of two macropulses of IR-laser light to the ion trap. Monitoring the abundances of the fragment ions formed as a function of the wavelength then provides an IR spectrum of the mass-selected ions. Because the fragmentation thresholds of the ions studied are much above the energy of a single IR photon in the spectral regime covered, several photons are required and thus the experiments are commonly referred to as infrared-multiphoton dissociation (IRMPD); note, however, that the process involves the sequential absorption of several photons, not the simultaneous action of multiple photons. In the 45 MeV range in which CLIO was operated during these experiments, the IR light covers a spectral range from about 1000 to about 2000 cm^{-1}. One data point of a typical IRMPD spectrum is derived from the average of four mass spectra (each with 8 accumulated microscans) per wavenumber, then the latter is changed with a step size of about 5 cm^{-1} and the next data point is taken. The typical acquisition time of an IRMPD spectra spanning a spectral range of about 1000 cm^{-1} is about an hour. Because of occasional instabilities of the combination of the IR laser and ESI-MS, all spectra at CLIO were at least taken two times, and the data shown below are the averages of these runs. Note that in this kind of action spectra, the assumption that the amount of ion fragmentation is proportional to the IR absorbance is not always justified because of the multiphotonic nature of IRMPD, and the major weight is therefore put on the peak positions rather than the peak heights in the IRMPD spectra.[39,40]

The calculations[41] were performed using the hybrid density functional method B3LYP[42−45] in conjunction with TZVP basis sets.[46] All reported structures represent minima on the potential-energy surface as revealed by the Hessian-matrix analysis at the same level of theory, and the same basis set which was also used for the prediction of (harmonic) vibrational frequencies. All calculations refer to the gaseous state in that additional solvation, aggregation, and so forth are deliberately not included. For comparison with the experimental infrared spectra, in agreement with common practice we use a uniform scaling factor of 0.975 for the calculated (harmonic) infrared frequencies.[47] Previous IRMPD studies

(29) (a) Roithová, J.; Ricketts, C. L.; Schröder, D.; Price, S. D. *Angew. Chem., Int. Ed.* **2007**, *46*, 9316. (b) Zins, E. L.; Schröder, D. *J. Phys. Chem. A* **2010**, *114*, 5989.

(30) Schröder, D.; Souvi, O.; Alikhani, E. *Chem. Phys. Lett.* **2009**, *470*, 162.

(31) (a) Ervin, K. M. *Chem. Rev.* **2001**, *101*, 391. (b) Rodgers, M. T.; Armentrout, P. B. *Acc. Chem. Res.* **2004**, *37*, 989. (c) Armentrout, P. B.; Ervin, K. M.; Rodgers, M. T. *J. Phys. Chem. A* **2008**, *112*, 10071; see also: (d) Narancic, S.; Bach, A.; Chen, P. *J. Phys. Chem. A* **2007**, *111*, 7006.

(32) (a) Schröder, D.; Engeser, M.; Schwarz, H.; Rosenthal, E. C. E.; Döbler, J.; Sauer, J. *Inorg. Chem.* **2006**, *45*, 6235. (b) Schröder, D.; Roithová, J.; Schwarz, H. *Int. J. Mass Spectrom.* **2006**, *254*, 197. (c) Schröder, D.; Roithová, J.; Gruene, P.; Schwarz, H.; Mayr, H.; Koszinowski, K. *J. Phys. Chem. A* **2007**, *111*, 8925. (d) Schlangen, M.; Neugebauer, J.; Reiher, M.; Schröder, D.; Pitarch López, J.; Haryono, M.; Heinemann, F. W.; Grohmann, A.; Schwarz, H. *J. Am. Chem. Soc.* **2008**, *130*, 4285. (e) Milko, P.; Roithová, J.; Schröder, D.; Lemaire, J.; Schwarz, H.; Holthausen, M. C. *Chem.—Eur. J.* **2008**, *14*, 4318. (f) Butschke, B.; Schlangen, M.; Schröder, D.; Schwarz, H. *Chem.—Eur. J.* **2008**, *14*, 11050. (g) Butschke, B.; Schlangen, M.; Schröder, D.; Schwarz, H. *Helv. Chim. Acta* **2008**, *91*, 1902. (h) Tyo, E. C.; Castleman, A. W., Jr.; Schröder, D.; Milko, P.; Roithová, J.; Ortega, J. M.; Cinellu, M. A.; Cocco, F.; Minghetti, G. *J. Am. Chem. Soc.* **2009**, *131*, 13009.

(33) For recent reviews of ion-mobility measurements of gaseous ions, see: (a) Kanu, A. B.; Dwivedi, P.; Tam., M.; Matz, L.; Hill, H. H., Jr. *J. Mass Spectrom.* **2007**, *43*, 1. (b) Bohrer, B. C.; Mererbloom, S. I.; Koeniger, S. L.; Hilderbrand, A. E.; Clemmer, D. E. *Ann. Rev. Anal. Chem.* **2008**, *1*, 293. (c) Puton, J.; Nousiainen, M.; Sillanpaa, M. *Talanta* **2008**, *76*, 978.

(34) Reference 33a also includes a schematic drawing of the first SYNAPT generation.

(35) See: D'Agostino, P. A.; Chenier, C. L. *Rapid Commun. Mass Spectrom.* **2010**, *24*, 1617.

(36) Mac Aleese, L.; Simon, A.; McMahon, T. B.; Ortega, J. M.; Scuderi, D.; Lemaire, J.; Maitre, P. *Int. J. Mass Spectrom.* **2006**, *249*, 14.

(37) Chiavarino, B.; Crestoni, M. E.; Fornarini, S.; Lanucara, F.; Lemaire, J.; Maitre, P. *Angew. Chem., Int. Ed.* **2007**, *46*, 1995.

(38) Simon, A.; Aleese, L.; Maitre, P.; Lemaire, J.; McMahon, T. B. *J. Am. Chem. Soc.* **2006**, *129*, 2829.

(39) (a) Schröder, D.; Schwarz, H.; Milko, P.; Roithová, J. *J. Phys. Chem. A* **2006**, *110*, 8346. (b) Schröder, D.; Ducháčková, L.; Jušinski, I.; Eckert-Maksić, M.; Heyda, J.; Tůma, L.; Jungwirth, P. *Chem. Phys. Lett.* **2010**, *490*, 14.

(40) (a) Moore, D. T.; Oomens, J.; Eyler, J. R.; von Helden, G.; Meijer, G.; Dunbar, R. C. *J. Am. Chem. Soc.* **2005**, *127*, 7243. (b) Polfer, N. C.; Oomens, J.; Dunbar, R. C. *Phys. Chem. Chem. Phys.* **2006**, *8*, 2744.

(41) *Gaussian 03*, Revision E.01; Gaussian, Inc.: Wallingford, CT, 2004.

(42) Vosko, S. H.; Wilk, L.; Nusair, M. *Can. J. Phys.* **1980**, *58*, 1200.

(43) Lee, C.; Yang, W.; Parr, R. G. *Phys. Rev. B* **1988**, *37*, 785.

(44) Becke, A. D. *Phys. Rev. A* **1988**, *38*, 3098.

(45) Becke, A. D. *J. Chem. Phys.* **1993**, *98*, 5648.

(46) Schaefer, A.; Huber, C.; Ahlrichs, R. *J. Chem. Phys.* **1994**, *100*, 5829.

(47) Merrick, J. P.; Moran, D.; Radom, L. *J. Phys. Chem. A* **2007**, *111*, 11683.

of related 3d transition-metal complexes have amply justified the use of scaling.[12b,32e,48]

Results and Discussion

This work is focused on selected mononuclear $[(DMF)_nMCl]^+$ and dinuclear $[(DMF)_nM_2Cl_3]^+$ cations of the late 3d-transition-metals M = Co, Ni, Cu, and Zn, specifically, the ions with $n = 2$ for M = Co−Cu and those with $n = 3$ for M = Zn, where the different value of n in the case of zinc is a consequence of the dissociation behavior of the dinuclear species (see below). Before focusing on the collision-induced dissociation data as well as the gas-phase infrared spectra further below, the general behavior of dilute solutions of MCl_2 and DMF in methanol/water (1:1) upon ESI is outlined briefly. The divalent forms of the late transition metals show very close similarities in the distributions of ions formed upon ESI in the positive-ion mode. For millimolar solutions of the metal(II) chlorides in methanol/water with 1% DMF, good yields of the monocations $[(DMF)_nMCl]^+$ and $[(DMF)_nM_2Cl_3]^+$ are obtained upon ESI, where the value n is determined by the ionization conditions and intrinsic features of the complexes.[26] In general, for soft ionization conditions larger values of n are observed (see Experimental Details). The specific choice of n for the title ions is explained further below.

The major aim of this work is to gain insight into the DMF-ligated dinuclear cluster ions to understand the effect of small amounts of DMF on the association of the metal salts in the presence of small amounts of DMF. While the initial concentration of DMF in the aqueous feed solution will increase upon droplet shrinking because of the larger volatility of water compared to DMF, the used amounts of DMF appear much too small to significantly change the bulk properties of the solvent mixture.[49] Hence, the clustering might have a specific molecular origin, for example, favored formation of oligonuclear clusters via bridging ligands, which might be revealed by gas-phase experiments. To avoid being misled by the particularities of a single species, we have chosen the DMF complexes of the late 3d metals from Co^{II} to Zn^{II} for a parallel investigation. As the first experimental method, we have chosen collision-induced dissociation (CID) which can reveal the characteristics of dissociation, provide insight into the competition between thermodynamically and kinetically preferred pathways, and in the particular case of energy-resolved experiments also deliver energetic information.[31,32,50] As a second, method we use IRMPD spectroscopy of the mass-selected ions.[51] Both, CID and IRMPD involve ion dissociation and are yet highly complementary: the ionic fragments and their energy behavior are of major concern in CID experiments, whereas ion fragmentation only serves as a monitor IRMPD, where the attention is paid to the wavenumbers of the IR transitions sampled. In this respect it is important to note that IRMPD can only occur if the vibrational ground state of the molecule sampled absorbs the IR radiation. Hence, CID probes the fragment ions themselves as well as the dynamics in the course of fragmentation (e.g., kinetic versus thermochemical control), whereas IRMPD probes the infrared spectra of the ground-state species and thus indirectly the parent-ion structures.

With respect to the number of DMF ligands n in the title ions $[(DMF)_nMCl]^+$ and $[(DMF)_nM_2Cl_3]^+$, we have chosen the value of n for which the dinuclear species $[(DMF)_nM_2Cl_3]^+$ show a direct competition between DMF loss (reaction 1) and cluster degradation (reaction 2).

$$[(DMF)_nM_2Cl_3]^+ \rightarrow [(DMF)_{n-1}M_2Cl_3]^+ + DMF \quad (1)$$

$$[(DMF)_nM_2Cl_3]^+ \rightarrow [(DMF)_nMCl]^+ + MCl_2 \quad (2)$$

At the same time, the complexes have been investigated computationally with a focus on those values of n for which most experimental information is available. Accordingly, we have investigated $[(DMF)_2M_2Cl_3]^+$ for M = Co, Ni, and Cu, whereas in the case of M = Zn, only ions with $n = 3$ could be generated in yields sufficient for MS/MS experiments.[52] With regard to the corresponding mononuclear complexes serving as reference species, our experience gained in the past indicates that the average hydration numbers of microhydrated ions strongly depend on the net charge but to a much smaller extent from the number or metal atoms,[7c,10,53] and the same holds true for ligands other than water.[9−11] Therefore, the value of n selected for the binuclear species was adopted for the corresponding mononuclear complexes.

Collision-Induced Dissociation. Upon collisional activation of the mononuclear complexes $[(DMF)_nMCl]^+$, loss of neutral DMF prevails for all metals and values of n and is often observed exclusively. Additional fragmentation channels, such as loss of HCl, are observed for some of the $[(DMF)MCl]^+$ cations in small amounts which indicate the occurrence of C−H bond activation.[54] These channels are not pursued any further because of their low abundance with respect to the other fragments of the $[(DMF)_nMCl]^+$ and $[(DMF)_nM_2Cl_3]^+$ ions with $n = 2$ and 3.[55]

A notable exception is $[(DMF)_2CuCl]^+$, however. Unlike the cations derived from Co^{II}, Ni^{II}, and Zn^{II}, the formal Cu^{II} compound shows the loss of atomic chlorine as the lowest-energy fragmentation channel, whereas expulsion of a neutral DMF ligand only occurs at slightly elevated collision energies. The loss of atomic chlorine is associated with a reduction of copper ion from Cu^{II} to Cu^{I}. While this preferential cleavage of a covalent instead of a coordinative bond might appear surprising, it reflects the solvent-stabilization of higher oxidation states which vanishes upon sequential removal of ligands.[50,56] Particularly

(48) (a) Milko, P.; Roithová, J.; Tsierkezos, N. T.; Schröder, D. *J. Am. Chem. Soc.* **2008**, *130*, 7186. (b) Milko, P.; Roithová, J. *Inorg. Chem.* **2009**, *48*, 11734.

(49) See also:Gatlin, C. L.; Tureček, F. *Anal. Chem.* **1994**, *66*, 712.

(50) (a) Trage, C.; Diefenbach, M.; Schröder, D.; Schwarz, H. *Chem.—Eur. J.* **2006**, *12*, 2454. (b) Grüne, P.; Trage, C.; Schröder, D.; Schwarz, H. *Eur. J. Inorg. Chem.* **2006**, 4546.

(51) Recent reviews: (a) Dopfer, O. *J. Phys. Org. Chem.* **2006**, *19*, 540. (b) Polfer, N. C.; Oomens, J. *Phys. Chem. Chem. Phys.* **2007**, *9*, 3804. (c) Asmis, K. R.; Sauer, J. *Mass Spectrom. Rev.* **2007**, *26*, 542. (d) MacAleese, L.; Maitre, P. *Mass Spectrom. Rev.* **2007**, *26*, 583.

(52) Traces of $[(DMF)_2Zn_2Cl_3]^+$ with the correct isotope pattern and consistent mass (exp. 378.7816, calc. 378.7804) were observed at elevated cone voltages, but neither CID nor IRMPD studies were possible.

(53) (a) Jagoda-Cwiklik, B.; Jungwirth, P.; Rulíšek, L.; Milko, P.; Roithová, J.; Lemaire, J.; Maitre, P.; Ortega, J. M.; Schröder, D. *ChemPhysChem* **2007**, *8*, 1629. (b) Schröder, D.; de Jong, K. P.; Roithová, J. *Eur. J. Inorg. Chem.* **2009**, 2121.

(54) For a recent review of C-H bond activation by gaseous metal ions, see: Roithová, J.; Schröder, D. *Chem. Rev.* **2010**, *110*, 1170.

(55) In the case of nickel, previous labeling data for $[(DMF)_nNiCl]^+$ complexes imply C-H bond activation of one of the *N*-methyl groups rather than of the formyl unit CHO in DMF; see ref 9.

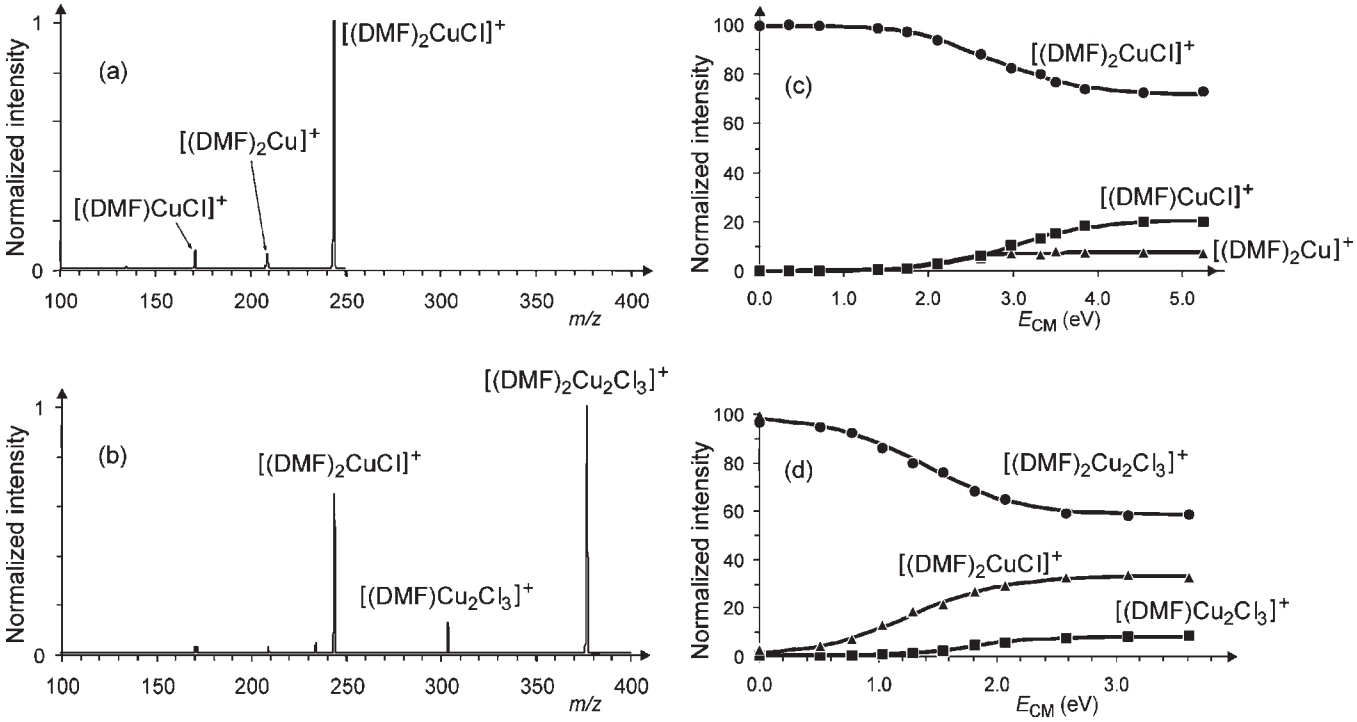

Figure 1. Representative CID spectra (both at ca. 2.5 eV collision energy in the center-of-mass frame) of mass-selected DMF complexes of late 3d-metal chloride cations: (a) $[(DMF)_2CuCl]^+$ and (b) $[(DMF)_2Cu_2Cl_3]^+$. The panels (c) and (d) display the energy behavior of the primary fragmentation channels for both ions, that is, the relative abundances of the parent- and fragment ions as a function of collision energy. Note that because of the approximate single-collision-conditions applied, significant fractions of the parent ions do not dissociate at elevated collision energies.

in the case of gaseous Cu^{II} complexes, this behavior is in fact quite common for trisligated complexes $[(L)_2CuX]^+$ (X = monovalent counterion).[32e,57,58]

For the dinuclear clusters, a competition between loss of neutral DMF (reaction 1) and cluster degradation (reaction 2) is observed, of which reaction 2 makes a connection between the mono- and binuclear ions. In this context, we note that the spin multiplicities of the electronic ground states of neutral metal(II) halides, that is, $CoCl_2$ ($^4\Sigma_g^-$), $NiCl_2$ ($^3\Sigma_g^-$), $CuCl_2$ ($^2\Pi_g$), $ZnCl_2$ ($^1\Sigma_g^-$),[59] do not give any indications for putative kinetic bottlenecks associated with spin inversion in ion dissociation according to reaction 2.[60]

As examples for the data and their analysis, the CID spectra of mass-selected $[(DMF)_2CuCl]^+$ and $[(DMF)_2Cu_2Cl_3]^+$ are shown in Figure 1 together with breakdown diagrams illustrating the energy behavior of the primary channels. Figure 1a (taken at a collision energy of 2.5 eV in the center-of-mass frame) shows the competition of the loss of DMF as the dominating channel (reaction 3) with the expulsion of atomic chlorine according to reaction 4, which corresponds to a reduction of the formal copper(II) precursor to copper(I).[57] Although less abundant at most collision energies, the loss of $Cl^\bullet$ has a lower appearance energy, that is, $AE(3) = 2.1$ eV versus $AE(4) = 1.7$ eV. The fact that it cannot efficiently compete with the loss of DMF above the threshold of the latter may be seen as an indication of a kinetic hindrance imposed by the geometrical changes of the ligand environment when going from Cu^{II} (with usually tetrahedral or octahedral coordination) to Cu^I, which typically forms bisligated, linear complexes.[58]

$$[(DMF)_2CuCl]^+ \rightarrow [(DMF)CuCl]^+ + DMF \quad (3)$$

$$[(DMF)_2CuCl]^+ \rightarrow [(DMF)_2Cu]^+ + Cl^\bullet \quad (4)$$

As shown in Figure 1b (also taken at a collision energy of 2.5 eV in the center-of-mass frame), the corresponding dinuclear cluster $[(DMF)_2Cu_2Cl_3]^+$ does not undergo a similar reduction process, but instead either loses neutral DMF or dissociates into a mononuclear copper complex via a loss of neutral $CuCl_2$ (reactions 1 and 2 with M = Cu and $n = 2$). The latter process has the lower *AE* and dominates the CID pattern over the entire energy range. Accordingly, two DMF ligands are the critical size for the stability of the dinuclear cluster upon sequential desolvation in the gas phase for M = Cu. In other words, the loss of DMF predominates for larger *n*, whereas cluster degradation to mononuclear species prevails for $n = 2$; this is consistent with the observation that only negligible

(56) (a) Stace, A. J. *Phys. Chem. Chem. Phys.* **2001**, *3*, 1935. (b) Stace, A. J. *J. Phys. Chem. A* **2002**, *106*, 7993.

(57) (a) Hao, C.; March, R. E. *J. Mass. Spectrom.* **2001**, *36*, 509. (b) Seymour, J. L.; Tureček, F. *J. Mass Spectrom.* **2002**, *37*, 533. (c) Schröder, D.; Holthausen, M. C.; Schwarz, H. *J. Phys. Chem. B* **2004**, *108*, 14407. (d) Tintaru, A.; Charles, L.; Milko, P.; Roithová, J.; Schröder, D. *J. Phys. Org. Chem.* **2009**, *22*, 229. (e) Tsierkezos, N. G.; Buchta, M.; Holý, P.; Schröder, D. *Rapid Commun. Mass Spectrom.* **2009**, *23*, 1550. (f) Révész, Á.; Milko, P.; Žabka, J.; Schröder, D.; Roithová, J. *J. Mass Spectrom.* **2009**, *45*, 1246.

(58) For recent reviews about the gas-phase chemistry of copper, see: (a) Tureček, F. *Mass Spectrom. Rev.* **2007**, *26*, 563. (b) Roithová, J.; Schröder, D. *Coord. Chem. Rev.* **2009**, *253*, 666.

(59) Hargittai, M. *Chem. Rev.* **2000**, *100*, 2233.

(60) (a) Detrich, J. L.; Reinaud, O. M.; Rheingold, A. L.; Theopold, K. H. *J. Am. Chem. Soc.* **1995**, *117*, 11745. (b) Schröder, D.; Shaik, S.; Schwarz, H. *Acc. Chem. Res.* **2000**, *33*, 139. (c) Schwarz, H. *Int. J. Mass Spectrom.* **2004**, *237*, 75. (d) Shaik, S.; Hirao, H.; Kumar, D. *Acc. Chem. Res.* **2007**, *40*, 532.

Table 1. Phenomenological Appearance Energies (*AEs*)[a,b] and Branching Ratios (*BRs*)[b] of the Major Fragments Observed upon CID of Mass-Selected, Mono- and Dinuclear Metal/DMF Complexes

	AE(-DMF)[c]	*BR*(-DMF)[c]	*AE*(other)	*BR*(other)	other losses
$[(DMF)_2CoCl]^+$	2.3	100			
$[(DMF)_2Co_2Cl_3]^+$	3.0	17	1.6	83	$-CoCl_2$
$[(DMF)_2NiCl]^+$	1.7	100			
$[(DMF)_2Ni_2Cl_3]^+$	2.5	17	1.3	83	$-NiCl_2$
$[(DMF)_2CuCl]^+$	2.1	74	1.7	26	$-Cl^{\bullet}$
$[(DMF)_2Cu_2Cl_3]^+$	2.4	19	0.6	81	$-CuCl_2$
$[(DMF)_2ZnCl]^+$	1.6	100			
$[(DMF)_3ZnCl]^+$	0.8	100			
$[(DMF)_3Zn_2Cl_3]^+$	1.0[d]	20	0.5	80	$-ZnCl_2$

[a] The experimental uncertainties of the derived *AE*s amount to ±0.1 eV. However, previous comparison with literature data revealed additional systematic errors of up to ±0.5 eV in the absolute values.[30,32,50] [b] Details about the procedure to determine the *AEs* are given in the Experimental Section. [c] Loss of a neutral DMF ligand from the parent ion. [d] Error enlarged to ±0.2 eV because of insecure assignment of the primary DMF loss to the common consecutive fragment $[(DMF)_2ZnCl]^+$ arising from both channels (see text).

amounts of $[(DMF)Cu_2Cl_3]^+$ are generated in the ESI source at harsher ionization conditions.

In Table 1, the appearance energies and the respective branching ratios of the ions studied are reported. Note that the *AE*s are derived from an extrapolation of the linear part of the rise of the fragment ions to the baseline and bear both systematic as well as statistical errors (see footnotes of Table 1). Instead of the exact thermochemical thresholds, the main purpose of the *AE*s is to (i) provide a simple description of the energy behavior of the various ions upon CID and (ii) allow comparisons between the different metals and the mononuclear as well as the dinuclear complexes.

Inspection of Table 1 reveals the following qualitative trends. (i) The appearance energies for the losses of DMF from the mononuclear ions $[(DMF)_nMCl]^+$ with $n = 2$ decrease from Co^{II} to Ni^{II}, increase again for Cu^{II}, and reach the lowest value for Zn^{II}. The somewhat larger *AE* in the case of $[(DMF)_2CuCl]^+$ may partially also be due to the neglect of the competitive shift by the less energy demanding loss of atomic chlorine.[61] The lowest *AE* for DMF loss is found for the mononuclear ion with $n = 3$ in the case of Zn^{II}, but this value cannot be compared directly because of the higher coordination number of the metal and thus easier ligand loss. (ii) For the dinuclear clusters, the *AEs* decrease continuously from Co^{II} to Cu^{II}; in the case of zinc, the analogous cluster $[(DMF)_2Zn_2Cl_3]^+$ could not be generated in the ion source, because loss of neutral $ZnCl_2$ from $[(DMF)_3Zn_2Cl_3]^+$ occurs already at low energies and is thus strongly preferred.[52] (iii) With the exception of M = Cu, loss of neutral DMF is observed exclusively for the mononuclear ions, whereas expulsion of MCl_2 is rather abundant for the dinuclear complexes. (iv) The *AE*s for the loss of neutral metal(II) chlorides from the dinuclear ions follow the trend of the DMF binding energies in that the *AE*s decrease from Co^{II} to Zn^{II}.

Computational Investigations. The mononuclear complexes investigated experimentally were additionally studied by means of DFT, and the results are summarized in Table 2. In all complexes, the electronic ground states of the diatomic MCl^+ cations[62] are maintained and coordination

Table 2. Selected Bond Lengths (Å), Vibrational Frequencies (cm^{-1}), and Calculated DMF-Binding Energies (in eV) of the Most Stable Isomers of the Mononuclear $[(DMF)_nMCl]^+$ Complexes for M = Co−Zn As Predicted by B3LZP/TZP Calculations[a]

	spin	r_{C-O}	r_{M-O}	r_{M-Cl}	ν_{sym}[b]	ν_{asym}[b]	*BDE*
$[(DMF)_2CoCl]^+$[c]	4	1.26	1.95	2.14	1707	1685	2.03
$[(DMF)_2NiCl]^+$	3	1.26	1.92	2.15	1704	1682	2.00
$[(DMF)_2CuCl]^+$[d]	2	1.27	1.89	2.20	1702	1683	2.82
$[(DMF)_2ZnCl]^+$[e]	1	1.27	1.94	2.15	1708	1692	1.91
$[(DMF)_3ZnCl]^+$[e]	1	1.25	2.00	2.23	1715	1687, 1688	1.33

[a] Unscaled frequencies. [b] These intense modes correspond to the carbonyl stretching of the coordinated DMF ligands. [c] For comparison: r_{M-O} = 2.13 Å in $[Co(DMF)_6]^{2+}$ in liquid phase.[64] [d] For comparison: r_{M-O} = 1.97/1.99 Å, r_{M-Cl} = 2.25/2.28 Å, and $r_{M-\mu-Cl}$ = 2.66 Å in crystalline dinuclear $[(DMF)_2(Cl)Cu(\mu\text{-}Cl)_2CuCl(DMF)_2]$.[65] [e] For comparison: r_{M-O} = 2.00 Å and r_{M-Cl} = 2.21 Å in crystalline $[(DMF)_2ZnCl_2]$.[65]

of the metal ion to the carbonyl-oxygen atom is highly preferred over bonding to the amide-nitrogen atom. The binding energies in $[(DMF)_2MCl]^+$ do not follow an obvious trend in that the BDEs are almost identical for M = Co and Ni, increase for M = Cu, and slightly decrease for M = Zn. Further, the corresponding properties of the $[(DMF)_3ZnCl]^+$ cation studied experimentally are given as well. Quite obviously, the computed binding energy of DMF in the complex $[(DMF)_3ZnCl]^+$ is smaller than in the $[(DMF)_2MCl]^+$ ions, fully consistent with the experimental data (Table 1). The marked increase of the BDE in the case of copper can be ascribed to the unfavorable situation in the resulting product $[(DMF)CuCl]^+$ in which the formal copper(II) center is only stabilized by a single DMF ligand. Likewise, the structure analysis of $[(DMF)_2CuCl]^+$ itself reveals that the Cu−O bonds are notably shorter than the corresponding bonds in all remaining $[(DMF)_2MCl]^+$ complexes, whereas the Cu−Cl bond is longer than all other M−Cl bonds. Thus, the large BDE of DMF results from its tight binding in $[(DMF)_2CuCl]^+$ and from a destabilization of the product. In marked contrast, the energy demand for loss of atomic chlorine is computed as only 1.66 eV for M = Cu, which is further supported by the experimental CID spectrum of the $[(DMF)_2CuCl]^+$ ion (Table 1). With exception of the copper complex, all relevant properties of the $[(DMF)_nMCl]^+$ ions are rather close to each other. Thus, the C−O distances of the carbonyl groups are almost identical, the M−O and M−Cl distances are very similar for all complexes and only for $[(DMF)_3ZnCl]^+$ having three DMF

(61) For a comprehensive analysis of the role of competitive shifts, see: Rodgers, M. T.; Armentrout, P. B. *J. Chem. Phys.* **1998**, *109*, 1787.

(62) For an extensive theoretical study and leading references, see: Yang, Y.; Weaver, M. N.; Merz, K. M. *J. Phys. Chem. A* **2009**, *113*, 9843.

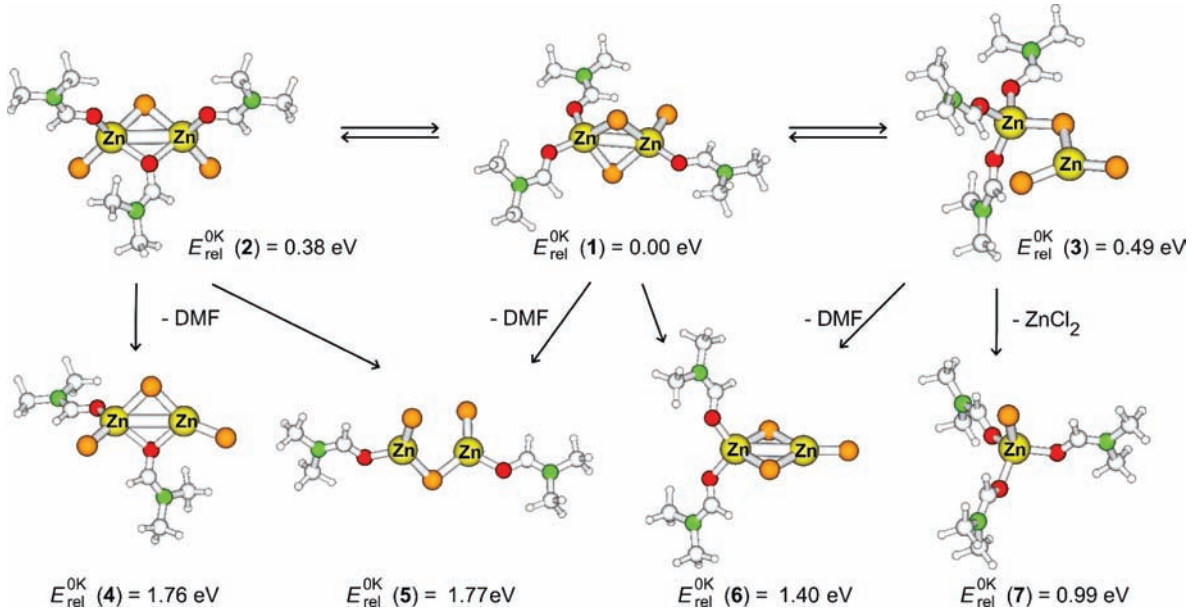

Figure 2. Competition between direct DMF losses from the lowest-energy isomer of the trisligated dinuclear cations, $[(DMF)_2Zn(\mu\text{-}Cl)_2Zn(Cl)(DMF)]^+$ (E_{rel}(**1**) = 0.00 eV), and its rearrangement into the isomeric clusters ions **2** and **3**, followed by loss of DMF to afford structures **4**–**6**, respectively. Alternatively, the formal contact ion pair **3** can also lose neutral $ZnCl_2$ to afford the mononuclear species **7**, which represents the least energy demanding pathway. Color code: Yellow, orange, red, and green correspond to zinc, chlorine, oxygen, and nitrogen, respectively.

ligands slight changes occur. Of importance for the interpretation of the IRMPD data discussed further below is that the symmetric and antisymmetric stretching modes of the coordinated amide are rather similar for the complexes of all four metal chlorides.[63]

With regard to the dinuclear complexes, the calculations are perturbed by the spin manifold arising for covalently bridged open-shell clusters of 3d metals. While DFT can be used to compute the dinuclear species, the reliability of the results for the different spin states is difficult to assess.[66] To stay on the safe side, we accordingly restrict the computational survey to the dinuclear complexes of zinc, for which only singlet multiplicity can be expected.

Figure 2 shows the lowest-energy structures found for the dinuclear zinc complexes with two and three DMF ligands. In the most stable structure of $[(DMF)_3Zn_2Cl_3]^+$, two μ-chloro bridges connect the zinc atoms, of which one is solvated by two DMF ligands whereas the other carries a DMF and a chloro ligand, that is, $[(DMF)_2Zn(\mu\text{-}Cl)_2Zn(Cl)(DMF)]^+$ with a quasi-tetrahedral environment of both metal atoms (structure **1** in Figure 2). The similar structure **2**, in which a bridging chloro ligand and a terminal DMF are interchanged, is calculated to be 0.38 eV higher in energy; structures with *N*-coordinated DMF ligands are much higher in energy (see Supporting Information).[67] The isomeric structure **3** with all three DMF ligands on the same zinc atom, formally corresponding to a contact-ion pair (CIP)[68] of a $[(DMF)_3Zn]^{2+}$ dication with a $[ZnCl_3]^-$ anion, is 0.49 eV higher in energy. Interestingly, however, the situation is inverse in the ion with only two DMF ligands in that the formal contact-ion pair $[(DMF)_2Zn(\mu\text{-}Cl)_2ZnCl]^+$ (**6**) is 0.37 eV more stable than the symmetrical cluster $[(DMF)(Cl)Zn(\mu\text{-}Cl)Zn(Cl)(DMF)]^+$ (**5**) and 0.36 eV more stable than a complex with one DMF ligand bridging both zinc atoms (structure **4**). Accordingly, the preferred route for the loss of DMF from the cluster can occur directly from the most stable isomer $[(DMF)_2Zn(\mu\text{-}Cl)_2Zn(Cl)(DMF)]^+$ to $[(DMF)_2Zn(\mu\text{-}Cl)_2ZnCl]^+$ with a computed overall BDE of 1.40 eV for the loss of a DMF ligand from $[(DMF)_3Zn_2Cl_3]^+$. In contrast, the cluster degradation leading to $[(DMF)_3ZnCl]^+$ (structure **7** in Figure 2) and neutral $ZnCl_2$ is initialized by the rearrangement of the $[(DMF)_2Zn(\mu\text{-}Cl)_2Zn(Cl)(DMF)]^+$ cluster to the less stable CIP $[(DMF)_3Zn(\mu\text{-}Cl)ZnCl_2]^+$, from which the subsequent expulsion of neutral $ZnCl_2$ demands only 0.50 eV; 0.99 eV relative to the most stable isomer **1**.

Cluster degradation is predicted by theory to be less energy demanding than the elimination of DMF, which is consistent with the predominance of the $[(DMF)_3ZnCl]^+$ fragment at low collision energies (Figure 3). Consistent with experiment, direct loss of DMF to afford $[(DMF)_2Zn_2Cl_3]^+$ can occur as a competing process at elevated energies. However, the internal energy deposited in the parent ion can also lead to sequential fragmentations even without involvement of multiple collisions. Thus, the primary fragment ion $[(DMF)_2Zn_2Cl_3]^+$ can undergo loss of neutral $ZnCl_2$ and likewise $[(DMF)_3ZnCl]^+$ can loose DMF, such that both primary dissociation products afford

(63) More detailed analysis of the data in Table 2 indeed reveals several significant correlations (e.g., between r_{M-O} and ν_{sym} with $r^2 = 0.96$), but the total shift of 13 cm^{-1} between the extremes of $[(DMF)_2CuCl]^+$ with r_{M-O} = 1.89 Å and $[(DMF)_3ZnCl]^+$ with r_{M-O} = 2.00 Å is significantly smaller than the spectral resolution of the IRMPD peaks.

(64) Yokoyama, H.; Suzuki, S.; Goto, M.; Shinozaki, K.; Abe, Y.; Ishiguro, S. *Z. Naturforsch. A: Phys. Sci.* **1995**, *50*, 301.

(65) Suzuki, H.; Fukushima, N.; Ishiguro, S.; Masuda, H.; Ohtaki, H. *Acta Crystallogr., Sect. C* **1991**, *47*, 1838.

(66) For instructive discussions of the particularly notorious case of $Fe_2S_2^{-/0/+/2+}$, see: (a) Hübner, O.; Sauer, J. *J. Chem. Phys.* **2002**, *116*, 617. (b) Hübner, O.; Sauer, J. *Phys. Chem. Chem. Phys.* **2002**, *4*, 5234; see also: (c) Pykavy, M.; van Wüllen, C.; Sauer, J. *J. Chem. Phys.* **2004**, *120*, 4207.

(67) For DMF as a bridging ligand, see: Kurtaran, R.; Yildirim, L. T.; Azaz, A. D.; Namli, H.; Atakol, O. *J. Inorg. Biochem.* **2005**, *99*, 1937.

(68) Marcus, Y.; Hefter, G. *Chem. Rev.* **2006**, *106*, 4585.

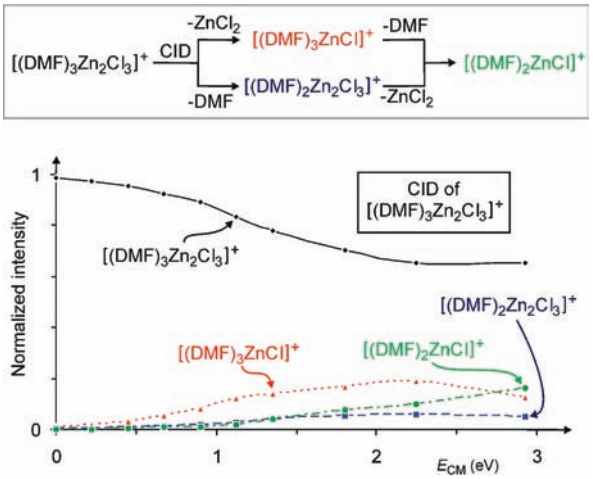

Figure 3. Fragment ions in the CID spectra of mass-selected $[(DMF)_3Zn_2Cl_3]^+$ as a function of the collision energy (given in eV in the center-of-mass scale). The inset on top shows the convergence of fragmentation channels for the dinuclear cluster.

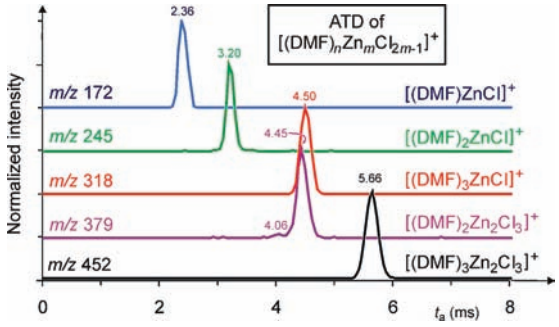

Figure 4. Arrival time distributions (ATDs) of the mass-selected mononuclear DMF complexes $[(DMF)ZnCl]^+$, $[(DMF)_2ZnCl]^+$, and $[(DMF)_3ZnCl]^+$ as well as the dinuclear clusters $[(DMF)_2Zn_2Cl_3]^+$ and $[(DMF)_3Zn_2Cl_3]^+$. Note that each ATD is normalized to the same height; in practice, the signal due to $[(DMF)_2Zn_2Cl_3]^+$ is less than 2 orders of magnitude less abundant than $[(DMF)_3Zn_2Cl_3]^+$. Further, note that the absolute arrival times (t_a) very much depend on the focusing conditions and gas flows in the ion-mobility instrument; thus, only the relative values are of relevance here.

$[(DMF)_2ZnCl]^+$ as a common fragment (see upper inset in Figure 3). In such a situation, the data cannot be deconvoluted unless reasonable assumptions about the energy-dependent branching can be made.[69]

Ion Mobility Studies. To seek for a more direct confirmation of the proposed existence of isomeric structures of the dinuclear cluster ions, we performed ion-mobility experiments concerning the zinc system on a recently installed SYNAPT G2 instrument. In ion-mobility experiments, mass-selected ions are guided through a drift tube in which a gas is present. Depending on both m/z ratio and ion structure, the ions reach the detector at different arrival times (t_a), where the major feature is the shape-sensitivity of the technique.[33] The results shown in Figure 4 reveal a continuous increase of the arrival times of the mononuclear $[(DMF)_nZnCl]^+$ ions with the number of DMF ligands n. A similar difference in arrival times occurs between the dinuclear clusters $[(DMF)_2Zn_2Cl_3]^+$ to $[(DMF)_3Zn_2Cl_3]^+$. With regard to ion mass, the dinuclear clusters have smaller arrival times than the mononuclear species, which can qualitatively be explained by the fact that addition of triatomic $ZnCl_2$ to $[(DMF)_2ZnCl]^+$ has a smaller effect on the overall size than that of a more bulky DMF ligand, where the latter is moreover associated by significant elongation of the coordinative bonds (Table 2). Thus, $[(DMF)_2Zn_2Cl_3]^+$ with m/z 379 has a slightly smaller arrival time than $[(DMF)_3ZnCl]^+$ with m/z 318. Interestingly, the arrival time distribution of mass-selected $[(DMF)_2Zn_2Cl_3]^+$ (m/z 378.781) shows a small second component at $t_a = (4.06 \pm 0.06)$ ms in addition to the major component with $t_a = (4.45 \pm 0.06)$ ms;[70] modeling with Gaussian functions suggest an about 1:30 ratio of the two components.[71,72] Observation of a minor isomer with lower mobility is fully consistent with the structures predicted for $[(DMF)_2Zn_2Cl_3]^+$ (Figure 2). The major component is assigned to structure **6**, $[(DMF)_2Zn(\mu\text{-}Cl)_2ZnCl]^+$, a contact ion pair with a significant dipole moment ($\mu_{calc} = 13.1$ D), which promotes the interaction with the gas present in the mobility unit. In contrast, the isomeric symmetrical structure **5**, $[(DMF)(Cl)Zn(\mu\text{-}Cl)Zn(Cl)(DMF)]^+$, is 0.37 eV higher in energy and has a significantly lower dipole moment ($\mu_{calc} = 4.5$ D) and is thus expected to have a smaller t_a. The third isomer **4**, $[(DMF)(Cl)Zn(\mu\text{-}Cl)(\mu\text{-}DMF)ZnCl]^+$, lying 0.36 eV above **6** and with a dipole moment of $\mu_{calc} = 9.9$ D, is neither expected to be resolved from the ATD of the predominating most stable isomer **6** nor expected to be formed in significant amounts upon CID of the parent ion having structure **1**.

Infrared Spectra. The IRMPD spectra of the mononuclear DMF complexes are summarized in Figure 5.[73] In the context of the vibrational spectroscopy of amides, it is useful to recall the nomenclature of the respective transitions, that is, the intense amide I band (1600−1700 cm^{-1}, primarily associated with the carbonyl stretching), the weaker amide II band between 1510−1580 cm^{-1} (NH_2 deformation), and the often complex amide III band due to the C−N stretch at about 1400 cm^{-1}. From comparison of the data it is obvious that the influence of the nature of the metal center on the infrared bands in the spectral region sampled is disappointingly small. Thus, all four spectra in Figure 5 bear an intense band at about 1370 cm^{-1}, with a shoulder at about 1440 cm^{-1}, and another intense band at about 1650 cm^{-1}, which is somewhat broadened for all metals with indications for band splitting in some cases.[74] The parallel theoretical treatment allows to assign the bands around 1650 cm^{-1} to the

(69) For a recent example of such a deconvolution, see: Couzijn, E. P. A.; Zocher, E.; Bach, A.; Chen., P. *Chem.—Eur. J.* **2010**, *16*, 5408.

(70) Although the second feature at $t_a = 4.06$ is not much above the noise level, it was fully reproducible in several independent ion-mobility scans and hence not just a spurious signal.

(71) Using the computed stability difference of 0.37 eV, treatment of the about 1:30 ratio using equilibrium considerations would suggest an effective temperature of about 1200 K which is within the range for ions formed via collision-induced dissociation (ref 72).

(72) Augusti, R.; Turowski, M.; Chen, H.; Cooks, R. G. *J. Mass Spectrom.* **2004**, *39*, 558.

(73) For a related IRMPD study of DMF complexes of alkyl zinc cations, see: Dreiocker, F.; Oomens, J.; Meijer, A. J. H. M.; Pickup, B. T.; Jackson, R. F. W.; Schäfer, M. *J. Org. Chem.* **2010**, *75*, 1203.

(74) A referee pointed out that increased widths of the peaks at about 1650 cm^{-1} could point to contributions of different rotamers, which indeed have very similar IR spectra. Because of the overall close similarities of the infrared patterns and the limited resolution of the IRMPD spectra, we refrain from a more detailed discussion of this aspect.

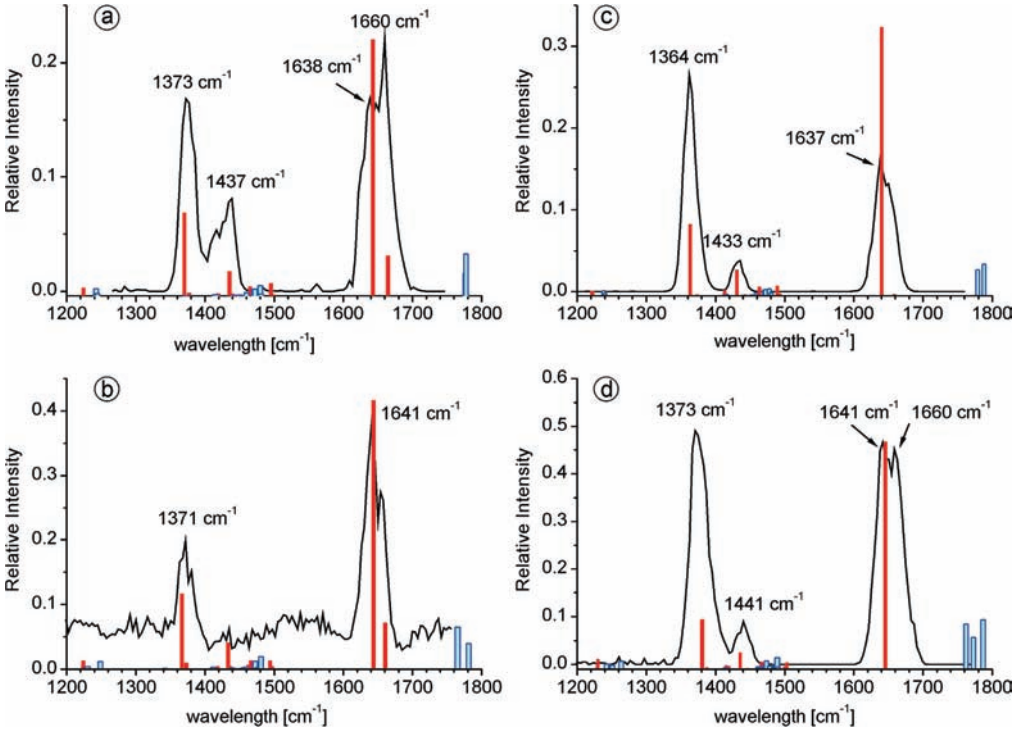

Figure 5. Measured IRMPD spectra in the fingerprint range (black lines) of the mononuclear DMF complexes (a) $[(DMF)_2CoCl]^+$, (b) $[(DMF)_2NiCl]^+$, (c) $[(DMF)_2CuCl]^+$, and (d) $[(DMF)_3ZnCl]^+$ and major bands predicted by theory for the O-coordinated structures (red bars) and the energetically less stable *N*-coordinated isomers (blue bars). The black numbers indicate the positions of the maxima in the experimental IRMPD data.

symmetric and asymmetric components of the amide I band of the coordinated DMF ligand (Table 2),[75] while the bands around 1400 cm^{-1} are mainly due to C−N stretching and thus resemble the amide III band. Linear scaling of the computed modes with 0.975 provides a reasonable agreement with the peak positions in the measured spectra (Figure 5). With respect to intensities we note that because of the multiphotonic nature of the IRMPD experiments the amount of ion fragmentation is not always proportional to the (single photon) IR absorbance, and the major weight is therefore put on the peak positions, rather than the peak heights in the IRMPD spectra.[39]

Very similar infrared patterns are obtained for the corresponding dinuclear cluster ions with M = Ni, Cu, and Zn (Figure 6); because of the close IR patterns, we did not record the IRMPD spectrum of the cobalt cluster. Further, we note that the energetically low-lying isomers of $[(DMF)_3Zn_2Cl_3]^+$ studied theoretically (Figure 2) cannot be distinguished via IRMPD in that peak positions as well as band intensities are almost superimposable. The isomeric structures **1** and **2** of $[(DMF)_3Zn_2Cl_3]^+$, for example, bear rather similar IR patterns despite the differences in geometry and coordination mode (see Figure 6c and 6d). Furthermore, regardless of the significant differences in the binding energies of the dinuclear clusters (Table 1), the IRMPD spectra of the $[(DMF)_nM_2Cl_3]^+$ ions are in fact by and large identical for M = Ni, Cu, and Zn as already found for the mononuclear complexes. We accordingly have to conclude that the infrared bands of the DMF ligands in IRMPD spectra cannot be used as sensitive probes for the coordination environment of these divalent 3d metal cations.[63]

Effect of DMF on the Cluster Formation. As outlined above, our initial speculation that DMF supports aggregation by acting as a favorable bridging ligand is not supported by the theoretical results. To further elucidate the situation, we investigated three aqueous solutions of identical $CuCl_2$ concentration and increasing DMF content. In the positive mode, the following types of ion were observed upon ESI: (i) hydrated copper complexes of the type $[(H_2O)_nCuX]^+$ with X = OH and Cl and average hydration numbers of $n_{av,OH} = 3.5$ and $n_{av,Cl} = 3.6$, respectively,[76] (ii) similar complexes in which one or more of the water ligands are replaced by DMF, that is, $[(DMF)(H_2O)_nCuX]^+$ with $n_{av,OH} = 1.6$ and $n_{av,Cl} = 1.8$ and $[(DMF)_2(H_2O)_nCuX]^+$ with $n_{av,OH} = 0.4$ and $n_{av,Cl} = 0.5$, (iii) $[(DMF)_3CuX]^+$ ions without additional water ligands and a pronounced preference for X = Cl in all samples, (iv) the dications $[(DMF)_nCu]^{2+}$ with $n = 4$ and 5, whereas dications containing water and DMF are almost absent, even for the lowest DMF content, and (v) binuclear clusters of the type $[(DMF)_{3-n}(H_2O)_nCu_2X_3]^+$. While the average hydration numbers derived from experiment strongly depend on the ionization conditions, at reasonably soft conditions they represent a measure for

(75) In Figure 5c (spectrum of $[(DMF)_2CuCl]^+$), there are also two peaks near 1650 cm^{-1} in analogy to 5a and 5b, but the second one at 1660 cm^{-1} has very low intensity. Likewise $[(DMF)_3ZnCl]^+$ has two bands in this region, but they are only 1 cm^{-1} apart so they appear as one band in Figure 5d. In addition, $[(DMF)_3ZnCl]^+$ has a third band coming from the combination of the amide vibrations of the three DMF ligands, which is 26 cm^{-1} blue-shifted, but its intensity is almost zero and therefore is not visible in the Figure.

(76) The average hydration number of a cation $[L_mMX(H_2O)_n]^+$ is calculated as $n_{av} = \sum(n_i \times I(n))/\sum I(n)$, where $I(n)$ stands for the abundance of a hydrated ion with n water ligands; see refs 7c, 10, and 53b.

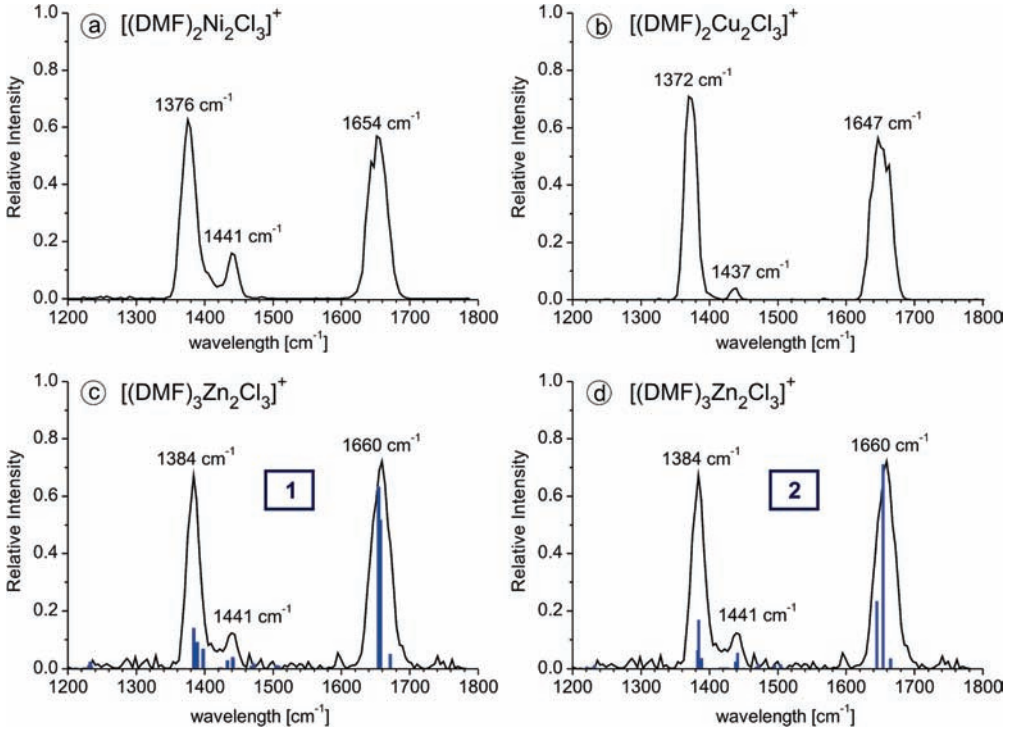

Figure 6. Measured IRMPD spectra in the fingerprint range of the dinuclear DMF complexes (a) $[(DMF)_2Ni_2Cl_3]^+$, (b) $[(DMF)_2Cu_2Cl_3]^+$, (c) and (d) $[(DMF)_3Zn_2Cl_3]^+$. The numbers indicate the positions of the maxima in the experimental IRMPD data. In the case of the zinc complex, the major bands predicted by theory are indicated as vertical blue bars for (c) the chlorine-bridged complex **1** (see Figure 2) and (d) the DMF-bridged structure **2**.

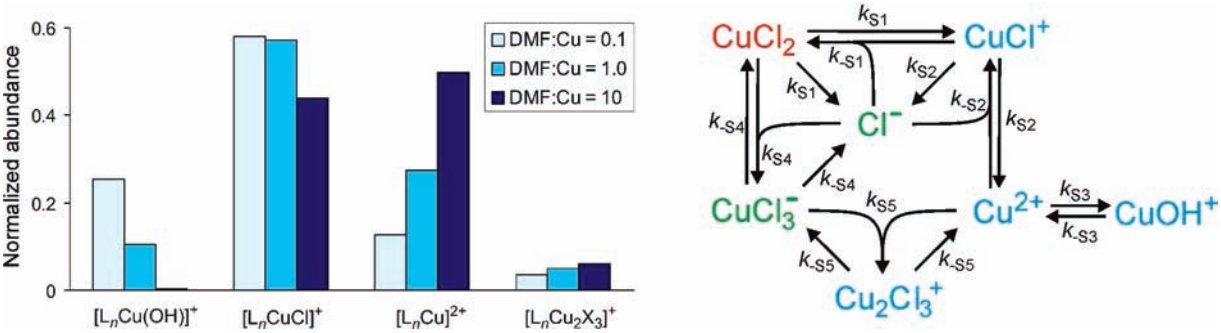

Figure 7. Normalized ion abundances of ligated copper cations in the ESI mass spectra of 0.005 molar $CuCl_2$ in water with different molar ratios of added DMF (DMF/Cu = 0.1, 1.0, and 10). For the sake of simplicity, all ligated species of a given core ion are summarized (i.e., L can be H_2O, DMF, or both, X in the dinuclear clusters stands for either OH or Cl). The scheme on the right-hand side shows the various equilibria involved; for details see Supporting Information.

the water affinity of the cationic cores.[7c,10,53] In line with earlier findings, incorporation of DMF in the monocationic species lowers the hydration numbers of the complexes by more than $\Delta n_{av} = 1$, which would be expected for the exchange of a monodentate ligand by another one.[10] The slightly, but significantly larger hydration numbers for X = Cl versus X = OH can be attributed to the electron withdrawing character of the chloro ligand, whereas the H-atom of the hydroxo ligand also can adopt part of the charge in a cationic species.[7c,53b,77] Because the resulting ESI mass spectra of aqueous $CuCl_2$ with traces of DMF are very rich in signals and moreover isobaric overlap of Cl and $(H_2O)(OH)$ subunits requires a deconvolution of the isotope patterns for quantitative analysis,[24,78] we present the results in a digested form (Figure 7) which shows the essential trends.

In addition to the obvious finding that the water ligands are easily replaced upon successive addition of DMF (not shown), the following trends can be extracted from Figure 7. The mixtures show a strong decrease of the hydroxo clusters $[L_nCu(OH)]^+$ with increasing DMF content which is compensated by a notable increase of the $[(DMF)_nCu]^{2+}$ dications. The fraction of the chloro complexes $[L_nCuCl]^+$ remains approximately constant. The abundance of the dinuclear clusters gently rises with increasing DMF content.[79] While the increase of the

(77) Schröder, D.; Schwarz, H. *Int. J. Mass Spectrom.* **2003**, *227*, 121.
(78) (a) Míšek, J.; Tichý, M.; Stará, I. G.; Starý, I.; Schröder, D. *Collect. Czech. Chem. Commun.* **2009**, *74*, 323. (b) Míšek, J.; Tichý, M.; Stará, I. G.; Starý, I.; Roithová, J.; Schröder, D. *Croat. Chem. Acta* **2009**, *82*, 79.

(79) The total ion currents were comparable for all three samples, which is consistent with the fact that at feed concentrations in the order of 10^{-3} mol L^{-1} the total ion current in the ESI is charge-limited. See also: Gatlin, C. L.; Tureček, F. *J. Mass Spectrom.* **2000**, *35*, 172.

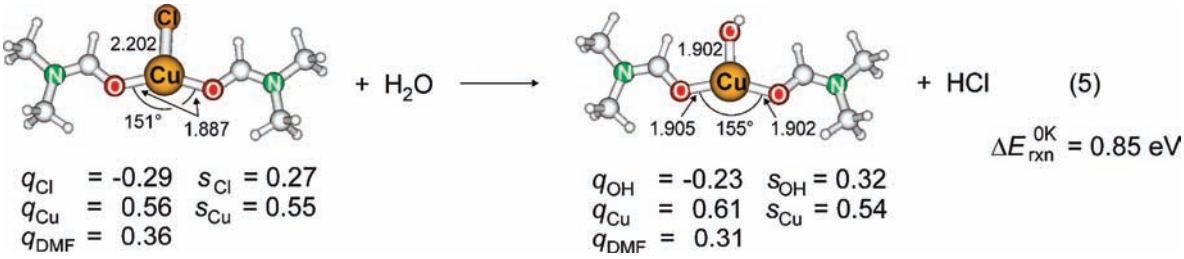

Figure 8. Hydrolysis of $[(DMF)_2CuCl]^+$ into $[(DMF)_2CuOH]^+$ according to reaction (5) and the calculated structures of the DMF complexes with some selected bond lengths (Å), angles (deg), and computed partial charges (q in e) and spin densities on copper, chlorine, and the hydroxy group, s_{Cu}, s_{Cl}, and s_{OH}, respectively.

$[(DMF)_nCu]^{2+}$ dications is consistent with condensed-phase data[80] and the previous indications of a DMF-promoted clustering were one of the motivations for this study,[10] it seems quite surprising that addition of a neutral ligand drastically influences the ratio between the copper-hydroxo and -chloro complexes. To rationalize these trends, we apply a phenomenological kinetic modeling[81] based on heterolysis as well as ion association and clustering in solution (for details see Supporting Information). With respect to the initial question about DMF-assisted clustering, the modeling suggests a complex interplay of various ion equilibria. Specifically, DMF stabilizes Cu^{2+} and thereby increases the amount of complete heterolysis to yield $[(DMF)_nCu]^{2+}$, going in hand with an increase of Cl^-. The latter, in turn, can associate with non-dissociated neutral $CuCl_2$ to yield the chlorocuprate(II) ion $CuCl_3^-$, which is the precursor for the dinuclear species via clustering with $[(DMF)_nCu]^{2+}$. The increased amount of clustering in the presence of DMF is thus not due to a direct stabilization of the clusters, but rather evolves as an indirect consequence of the increased concentrations of the cluster precursors.

It remains to be asked, why the presence of DMF so much suppresses the formation of the hydroxo complexes in favor of the chloro complexes. Besides the interplay of the various equilibria as revealed by the kinetic modeling, coordination of Cu^{II} by a chloride counterion appears to be preferred significantly compared to that by a hydroxide, when DMF is present. To probe this particular aspect, the enthalpy of reaction (5) has been calculated by DFT and found to be endothermic by as much as 0.85 eV (Figure 8). Hence, DMF leads to a large thermochemical preference of the chloro complex in comparison to the hydroxo complex.

The overall geometries of the chloro- and hydroxo-complexes $[(DMF)_2CuX]^+$ with X = Cl, OH (Figure 8) are rather similar and correspond to the trigonal-planar arrangement expected for a Cu^{II} compound with three ligands. However, the Cu−O distances to the O-atoms of the DMF ligands are significantly shorter for X = Cl than for X = OH. In part this certainly is a consequence of the larger Cu−X distance for X = Cl as a third-row atom, which reduces steric repulsion between the DMF ligands and the chloro ligand as compared to X = OH. However, some contribution from the charge on X (i.e., $q_{Cl} = -0.29$ versus $q_{OH} = -0.23$) is obvious, which results in a larger positive charge on the entire $[(DMF)_2Cu]$ fragment and hence also on the DMF ligands (i.e., $q_{DMF} = 0.36$ for X = Cl versus 0.31 for X = OH). These findings reiterate that for non-solvated metal cations a chlorine atom acts as a strong electron-withdrawing ligand which increases the positive charge on the metal center, whereas in a hydroxo ligand also the proton can carry part of the positive charge.[7c,30,53b,77,82] While for hydrated complexes $[(H_2O)_nMX]^+$ this may lead to a preference for the complexes with X = OH, the strong donor ability of DMF inverts this trend by stabilizing a high charge on the metal center such that $[(DMF)_nMCl]^+$ is preferred over $[(DMF)_nMOH]^+$.

Conclusions

The coordination of the formally divalent metal chloride ions MCl^+ of the late 3d transition metals from cobalt through zinc to DMF is probed in the gas phase by experiment and theory including infrared spectra of mass-selected ions. In addition to the mononuclear ions $[(DMF)_nMCl]^+$, also binuclear clusters of the type $[(DMF)_nM_2Cl_3]^+$ are considered. While the gross features of the $[(DMF)_nMCl]^+$ and $[(DMF)_nM_2Cl_3]^+$ ions are quite similar, several differences are notable. Thus, the binding energies of the DMF ligands as well as the energy demands for cluster cleavage both show the tendency to decrease from cobalt to zinc. The copper complex $[(DMF)_2CuCl]^+$ is an exceptional case because for this metal, and only for this one, a loss of atomic chlorine and thus reduction to Cu(I) is observed as the preferred dissociation pathway. Further, theory predicts the existence of isomeric cluster ions in the case of zinc, for example, the formal contact ion-pair $[(DMF)_2Zn(\mu\text{-}Cl)\text{-}ZnCl_2]^+$, with both DMF ligands on a single metal atom, and the alternative structure $[(DMF)(Cl)Zn(\mu\text{-}Cl)Zn(Cl)(DMF)]^+$ with a DMF ligand on each metal. Consistent with theory, exploratory ion-mobility studies of mass-selected $[(DMF)_2\text{-}Zn_2Cl_3]^+$ provide experimental evidence for the existence of these isomers. With regard to the spectroscopic features in the fingerprint region of the infrared spectrum, our studies reveal that the otherwise very useful IRMPD technique does not allow a clear-cut distinction between different isomeric structures because the spectral signatures for the different metals are almost identical. Nevertheless, in conjunction with theory

(80) Spah, M.; Spah, D. C.; Park, J. J.; Song, H.-J.; Park, K.; Park, J.-W. *Fluid Phase Equilib.* **2008**, *272*, 75.

(81) (a) Schröder, D.; Schwarz, H. *Angew. Chem., Int. Ed. Engl.* **1990**, *29*, 1431. (b) Schröder, D.; Brown, R.; Schwerdtfeger, P.; Schwarz, H. *Int. J. Mass Spectrom.* **2000**, *203*, 155. (c) Loos, J.; Schröder, D.; Zummack, W.; Schwarz, H.; Thissen, R.; Dutuit, O. *Int. J. Mass Spectrom.* **2002**, *214*, 105. (d) Butschke, B.; Schlangen, M.; Schwarz, H.; Schröder, D. *Z. Naturforsch., B: Chem. Sci.* **2007**, *62b*, 309. (e) Ricketts, C. L.; Schröder, D.; Alcaraz, C.; Roithová, J. *Chem.—Eur. J.* **2008**, *14*, 4779.

(82) Ončák, M.; Schröder, D.; Slavíček, P. *J. Comput. Chem.* **2010**, *31*, 2294.

the IRMPD spectra do not indicate any particular stabilizing effect of DMF upon the formation of dinuclear metal clusters. Instead, an analysis of the effects of minor DMF amounts on the ESI mass spectra of aqueous $CuCl_2$ reveals that the increased abundance of cluster ions results from shifts in the complex equilibria involved in favor of cluster precursors $[(DMF)_nCu]^{2+}$ and $CuCl_3^-$. While it is obvious that a consideration of the ESI mass spectra in terms of simple equilibria cannot account for the highly dynamical, non-equilibrium processes occurring upon ESI,[5,26,83] consideration of such equilibria can provide a qualitative understanding of ESI mass spectra with respect to the multiply coupled processes involved in solution chemistry. Specifically, ESI can be used to identify molecular species possibly involved in solution equilibria, thereby circumventing some complications which arise in the deconvolution of bulk properties.[84] However, the gap from the qualitative molecular insight obtained to the quantitative analysis of ESI spectra with regard to solution chemistry remains considerable and likewise a challenge. With regard to the DMF complexes studied here, the IRMPD technique appears to be of limited sensitivity for the distinction of mono- and oligomeric metal complexes and even for the differentiation between different metals. In this respect, additional spectroscopic methods exploring not only rovibronic, but also electronic transitions[85] appear as particular promising for the gas-phase characterization of reactive intermediates in transition-metal chemistry.

Acknowledgment. This work was supported by the Czech Academy of Sciences (Z40550506), the European Research Council (AdG HORIZOMS), the Grant Agency of the Czech Republic (203/08/1487), and the Ministry of Education of the Czech Republic (MSM0021620857). Further, we kindly appreciate the allocation of beam time at the IR laser center CLIO (IC 013-09), thank the entire team of CLIO for helpful assistance, and acknowledge travel support to CLIO within the TNA scheme of the European Commission. Last but not least, we thank the unknown referees for their constructive criticism.

Supporting Information Available: Details of the kinetic modeling, breakdown diagrams of all ions and Cartesian structures of the computed structures. This material is available free of charge via the Internet at http://pubs.acs.org.

(83) Luedtke, W. D.; Landman, U.; Chiu, Y.-H.; Levandler, D. J.; Dressler, R. A.; Sok, S.; Gordon, M. S. *J. Phys. Chem. A* **2008**, *112*, 9628.

(84) For a recent example of a comparison of solution phase NMR data and electrospray results about the aggregation of catalytically-active palladium complexes, see: Agrawal, D.; Schröder, D.; Sales, D. A.; Lloyd-Jones, G. *Organometallics* **2010**, *29*, 3979.

(85) (a) For a promising development in this respect, see: Svendsen, A.; Lorenz, U.; Boyarkin, O. V.; Rizzo, T. R. *Rev. Sci. Instrum.* **2010**, *81*, 073107. (b) Fedorov, A.; Couzijn, E. P. A.; Nagornova, N. S.; Boyarkin, O. V.; Rizzo, T. R.; Chen, P. *J. Am. Chem. Soc.* **2010**, *132*, 13789.